Journal of Alloys and Compounds, 206 (1994) 201–210
JALCOM 1037

Homogeneity ranges and thermodynamic properties of the Te-rich phases in the Cr–Te system

R. Viswanathan, M. Sai Baba, T.S. Lakshmi Narasimhan, R. Balasubramanian, D. Darwin Albert Raj and C.K. Mathews*
Materials Chemistry Division, Chemical Group, Indira Gandhi Centre for Atomic Research, Kalpakkam Tamil Nadu 603102 (India)

(Received November 2, 1993)

Abstract

The Te-rich region of the Cr–Te system was investigated by using high temperature mass spectrometry. The composition range from ~60 to 82.7 at.% Te was covered by preferentially evaporating off tellurium at $T<700$ K from the alloys of starting compositions 66.9, 70.1, 80.0 and 82.7 at.% Te. Evidence for the existence of a new polytelluride (77.0 ± 0.3 to 78.3 ± 0.2 at.% Te) was obtained while the existing uncertainty about the homogeneity range of $CrTe_3$, hitherto considered as the most Te-rich phase in the Cr–Te system, was removed. This phase exists from 70.5 ± 0.8 to 74.4 ± 0.5 at.% Te. In the case of Cr_5Te_8, only the Te-rich boundary (63.6 ± 0.6 at.% Te) could be deduced. The activities of tellurium across the single-phase regions were obtained from the $p(Te_2)$ measured as a function of composition and those of chromium computed by a Gibbs–Duhem integration. Subsequently Gibbs free energies of formation, $\Delta_f G_m^\circ$, at $T=650$ K were also deduced. The values (in kJ mol^{-1}, given in brackets) for the formulae (given in parentheses) corresponding to the Te-rich and/or Cr-rich boundary compositions are: $CrTe_{4-y}$ phase: $-[90.7\pm0.4]$ ($CrTe_{3.61}$) and $-[90.5\pm0.4]$ ($CrTe_{3.35}$); $CrTe_3$ phase: $-[90.4\pm1.0]$ ($CrTe_{2.91}$) and $-[89.5\pm1.5]$ ($CrTe_{2.39}$); Cr_5Te_8 phase: $-[86.2\pm2.2]$ ($CrTe_{1.75}$, the Te-rich boundary).

1. Introduction

In continuation of our high temperature mass spectrometric (HTMS) investigations on the Cr-rich region [1], we studied the Te-rich region of the Cr–Te system. There is considerable uncertainty in this region (above 60 at.% Te) as to the number of phases and their phase widths. To our knowledge, there exist mainly three studies in this region: They are:

(a) e.m.f. measurements by Goncharuk and Lukashenko [2] on the alloys having 65, 69.8, 78.6 and 88.6 at.% Te in the temperature range 623–723 K;
(b) X-ray and differential thermal analysis (DTA) measurements by Gunia [3]; and
(c) X-ray, DTA, and vapor pressure measurements by Ipser and co-workers [4–6].

Goncharuk and Lukashenko [2] concluded that the compositions studied by them, *i.e.* from 65 to 88.6 at.% Te all corresponded to a two-phase region. By assuming this two-phase region to be (Cr_2Te_3+Te), that is, by taking $a_{Te}=1$, they derived thermodynamic properties for Cr_2Te_3 from the measured chromium activities. Such an assumption obviously implies that no other phase which is more Te-rich than Cr_2Te_3 exists in the Cr–Te system. Gunia's [3] phase diagram shows the existence of one more telluride phase, Cr_3Te_8 (~72.5 at.% Te) beyond Cr_2Te_3 (~60 at.% Te) at $T<723$ K. On the contrary, the phase diagram proposed by Ipser *et al.* [6] shows the presence of two phases beyond Cr_2Te_3 (59.5–60.0 at.% Te): Cr_5Te_8 (60.5–62 at.% Te) and a polytelluride phase $CrTe_3$ (~75 at.% Te). These authors could not, however, ascertain whether the $CrTe_3$ phase had a range of homogeneity from 71 to 75 at.% Te or a new, though structurally closely related phase was formed at 70 at.% Te. They also disagreed with Gunia's conclusion that Cr_5Te_8 exists only at high temperatures.

In the present study, we covered the full composition range from ~60 to 82.7 at.% Te by starting with four samples of initial composition, 82.7, 80.0, 70.1 and 66.9 at.% Te and preferentially evaporating off Te during the course of HTMS measurements, in order to delineate phase boundaries. In one experiment, composition down to ~50 at.% Te was covered. This approach was successfully employed in our earlier studies on different M–Te systems where M≡Fe [7], Cr [1] and Mo [8]. Gibbs free energies of formation of the phases identified were also subsequently deduced.

*Author to whom correspondence should be addressed.

SSDI 0925-8388(93)01037-5

2. Experimental details

The samples of Cr–Te alloys were prepared by direct reaction of the elements. The required amounts of the two powders (to obtain the compositions 66.9, 70.1, 80.0 and 82.7 at.% Te) were mixed intimately, pelletized and placed inside quartz tubes. Before being sealed under vacuum ($\sim 1\times10^{-4}$ Pa), any air in the quartz tubes containing sample pellets was removed by repeatedly filling them with high purity argon followed by evacuation. They were heated at 675 K for about a month and cooled to ambient temperature. The contents in the tubes were ground well, repelletized and the heating cycle was repeated for an almost equal duration as the initial heating to make sure that equilibrations were complete. The final cooling to ambient temperature was done in steps of $\sim$20 K to allow equilibration at each temperature (maintained for a minimum period of $\sim$1 h) and to minimize the condensation of any tellurium vapor over the samples prepared.

A Knudsen cell mass spectrometer supplied by VG Micromass (model MM 30 BK) was used to conduct the vaporization studies. Knudsen cells made of alumina (height: 10 mm; inner diameter: 7.5 mm; orifice diameter: 0.5 mm) were used for containing the samples. The Knudsen cell was kept inside a tungsten cup which was heated by means of electron bombardment from two independent tungsten filaments. Temperatures were measured by a (chromel-to-alumel) thermocouple inserted through the base of the tungsten cup. The thermocouple was calibrated against the melting temperature of silver. More details of the instrument can be found elsewhere [7–9].

The molecules effusing from the Knudsen cell were ionized with 38 eV electrons. The ions generated were then accelerated to a potential of 6 kV and subsequently analyzed by a 90° sector, single focusing magnetic analyzer. The intensities of ions corresponding to different mass-to-charge ratios were measured by a secondary electron multiplier system. A shutter-plate which could be moved across the path of the molecular beam provided a method of distinguishing between the ions formed from the effusing vapor and those formed from the background gases in the ionization chamber. The ionic species were identified from the mass-to-charge ratios at which the "shutter effect" was seen, and by checking whether the net mass spectral peak heights were in reasonable accord with the isotopic abundance-distribution (known or calculated) for the ionic species.

Only tellurium ions and no chromium bearing ions were detected in the mass spectra. Obviously it is only the tellurium that vaporizes preferentially from these samples.

The experiments involved the continuous vaporization of samples (of known composition and weight) while at the same time monitoring the intensity of the ion Te_2^+. In all, nine runs were conducted: three runs with the 82.7 at.% Te sample (all at 650 K), three runs with the 80.0 at.% Te sample (two at 650 K, and one at 650 K as well as at different higher temperatures to force the sample to enter the most Cr-rich two-phase region at 1120 K), two runs with the 70.1 at.% Te sample (one at 650 K and the other at 688 K), and finally one run with the 66.9 at.% Te sample (at 650 K).

The total vapor pressure was always maintained below that ($\sim$10 Pa) required to meet the Knudsen flow conditions. Pressure calibrations were performed by vaporizing Te(s) before and after every experiment with a Cr–Te sample. The Knudsen cell (emptied of tellurium) was degassed at about 1300 K for a sufficiently long time to remove the traces of tellurium, if any, before charging a fresh Cr–Te sample into it.

Powder diffraction patterns of the starting elements as well as of samples prepared from them were taken by using the Cu Kα radiation (Siemens D500). Residues after some vaporization experiments were also subjected to X-ray diffraction analysis. The 2θ (Bragg) angles corresponding to the major peaks were measured precisely.

3. Results

Figures 1 and 2 show some typical $I(Te_2^+)\sqrt{T}$ *vs.* time plots. They correspond to the continuous vaporization experiments on samples of starting compositions 82.7 and 80 at.% Te, respectively. Effusion of tellurium vapor from the Knudsen cell resulted in the samples becoming progressively richer in chromium. As the vaporization proceeded, the sample traversed alternately through the single- and two-phase regions. The sample must have remained in the two-phase region(s) during the period(s) in which the $I(Te_2^+)$ was steady and in single-phase region(s) at other period(s) (*i.e.* when the intensity was changing). More meaningful information could be had by converting these to pressure–composition plots.

The partial pressure of Te_2, $p(Te_2)$, at temperature T was computed from the ion intensity, $I(Te_2^+)$, by employing the following equation:

$$p(Te_2) = kI(Te_2^+)T \tag{1}$$

where k is the pressure calibration constant, which was obtained by using the relation

$$k = \frac{p^\circ(Te_2)}{I^\circ(Te_2^+)T} \tag{2}$$

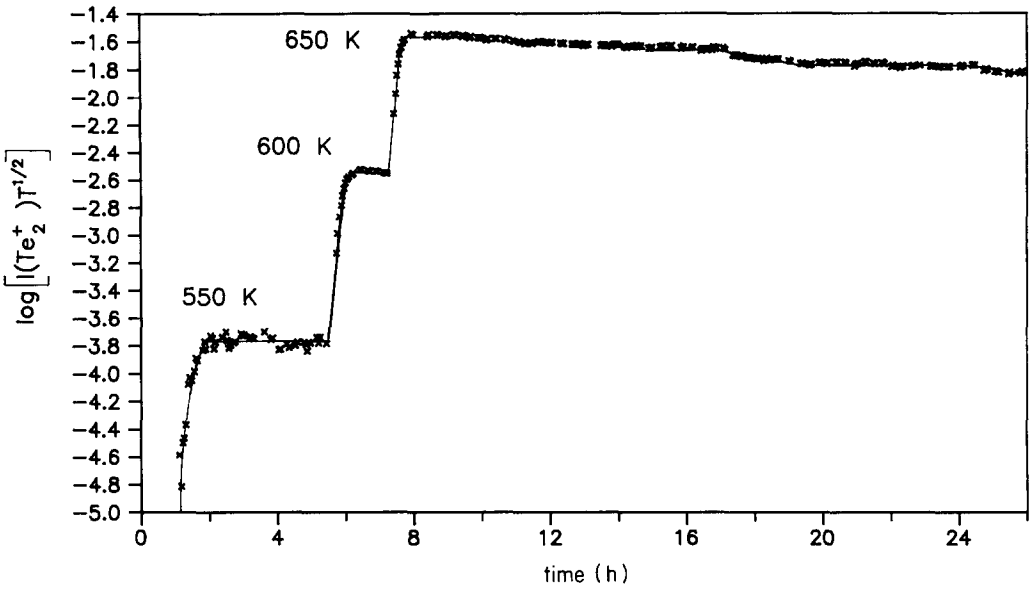

Fig. 1. $I(Te_2^+)$ as a function of time; starting composition of the sample: 82.7 at.% Te; initial weight: 0.202 62 g; total mass loss: 0.074 00 g.

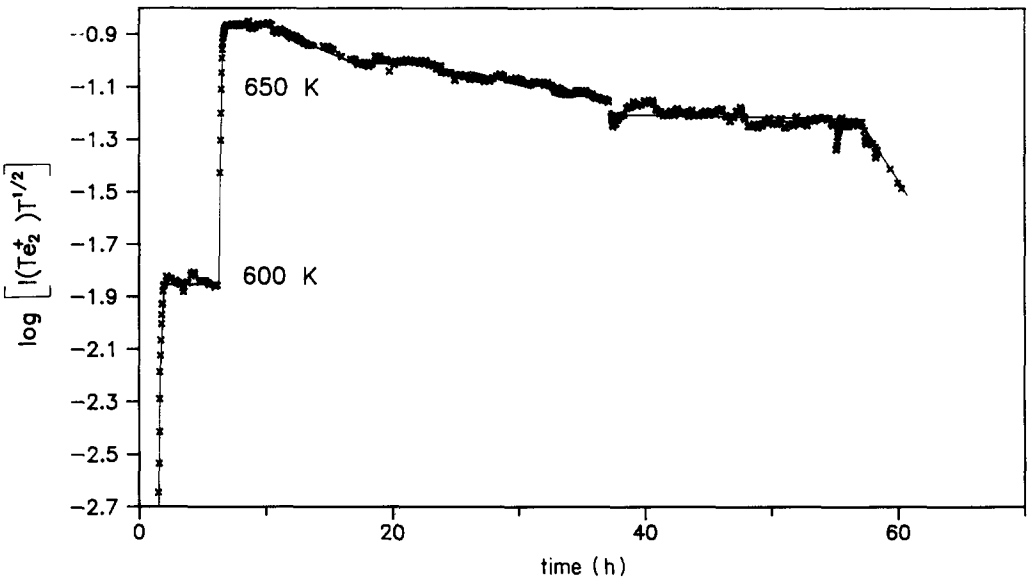

Fig. 2. $I(Te_2^+)$ as a function of time; starting composition of the sample: 80.0 at.% Te; initial weight: 0.333 00 g; total mass loss: 0.177 16 g.

The superscript "o" denotes that the $I(Te_2^+)$ and $p(Te_2)$ correspond to elemental tellurium.

The final composition of the sample in each experiment was computed from the total mass loss (due entirely to tellurium loss). The compositions at other points can be deduced by making use of the Hertz–Knudsen effusion equation:

$$\Delta W = \sum_i p(Te_i) \sqrt{\frac{M(Te_i)}{2\pi RT}}\, c_1\, \Delta t \qquad (3)$$

where ΔW is the total mass loss of the condensed phase, $p(Te_i)$ and $M(Te_i)$ are the partial pressures and the molar masses of different tellurium species Te_i, c_1 is the effective area of the Knudsen cell orifice ($c_1 = C \times A$ where C is the Clausing factor for the orifice whose area is A) and Δt is the duration for which the Knudsen cell was maintained at temperature, T. By combining the above equation with eqn. (2) and rearranging, the following equation was obtained, valid even for measurements done at different temperatures, T_j:

$$\Delta W = c_2 \left\{ \sum_j I(Te_2^+) \sqrt{T_j}\, \Delta t_j \left(1 + \sum_i Q_i\right) \right\} \qquad (4)$$

where

$$c_2 = (kc_1)[M(\mathrm{Te_2})/(2\pi R)]^{1/2} \quad (4a)$$

$$Q_i = \left[\sum_j r_i I(\mathrm{Te}_i^+)\sqrt{T_j}\,\Delta t_j\right] \Big/ \left[\sum_j I(\mathrm{Te_2}^+)\sqrt{T_j}\,\Delta t_j\right] \quad (4b)$$

and

$$r_i = (i/2)^{1/2}\,\frac{\sigma(\mathrm{Te_2})\gamma(\mathrm{Te_2}^+)n(\mathrm{Te_2}^+)}{\sigma(\mathrm{Te}_i)\gamma(\mathrm{Te}_i^+)n(\mathrm{Te}_i^+)} \quad (4c)$$

In the above equations, I^+ represents the intensity of ion corresponding to the vapor species Te_2 or Te_i ($i \neq 2$; *i.e.* $i = 1$–7 except 2), σ the ionization cross-section of the species, and γ and n the relative detector response and isotopic abundance of the ion, respectively.

Equation (4) can be employed only when intensity data (as a function of time) for all the tellurium ions are available. In the present study, only Te_2^+ (the ion representing the principal vapor species Te_2) was monitored. Therefore, the summation term $\Sigma_i Q_i$ was neglected (basis discussed in Section 4) and the following relation was used:

$$\Delta W = c_2' \sum_j I(\mathrm{Te_2}^+)\sqrt{T_j}\,\Delta t_j \quad (5)$$

The constant c_2' was first determined from the total mass loss and the total area under the $I(\mathrm{Te_2}^+)\sqrt{T}$ *vs.* time curve. Then by employing this, the mass loss up to (and thus also the composition at) any time could be readily computed from the corresponding area in the ($I\sqrt{T}$–time) plot.

Figures 3 and 4 represent the $p(Te_2)$ *vs.* composition plots derived from the $I(\mathrm{Te_2}^+)\sqrt{T}$ vs. time plots shown in Figs. 1 and 2. Four plateau regions (where $p(Te_2)$ remained constant) were identified. They are:

(a) plateau 1: $p(\mathrm{Te_2}) = p^\circ(\mathrm{Te_2}) = 1.5$ Pa at compositions above ~82 at.% of Te;
(b) plateau 2: $p(\mathrm{Te_2}) = \sim 1.2$ Pa from 78.3 ± 0.2 to 79.2 ± 0.5 at.% Te;
(c) plateau 3: $p(\mathrm{Te_2}) = \sim 0.9$ Pa from 74.4 ± 0.5 to 77.0 ± 0.3 at.% Te; and
(d) plateau 4: $p(\mathrm{Te_2}) = \sim 0.55$ Pa from 63.6 ± 0.6 to 70.5 ± 0.8 at.% Te.

The plateau regions represent two-phase mixtures while the regions between two plateaus (where the $p(Te_2)$ changed with composition) represent single-phase regions. A tentative formula, $CrTe_{4-y}$, has been assigned by us for the hitherto unknown single-phase between 77 and 78.3 at.% Te. The nominal formulae $CrTe_3$ and Cr_5Te_8 assigned by Ipser *et al.* [6] have, however, been retained to represent the two different phases at compositions less than 77 at.% Te.

Table 1 gives the composition ranges of these phases. The selected phase boundary compositions are the mean values. The experiments with 66.9 and 70.1 at.% Te samples were mainly used to confirm the Te-rich boundary of the Cr_5Te_8-phase, determined previously from investigations with the 80.0 at.% Te sample.

The $p(Te_2)$, determined as a function of composition, was converted to the activity of tellurium, a_{Te}, by employing the following equation:

$$a_{\mathrm{Te}} = [p(\mathrm{Te_2})/p^\circ(\mathrm{Te_2})]^{1/2} \quad (6)$$

where $p^\circ(Te_2)$ refers to the partial pressure of $Te_2(g)$ over elemental tellurium. The value of $p^\circ(Te_2)$ over solid tellurium at $T = 650$ K was computed from the relation given in ref. 9:

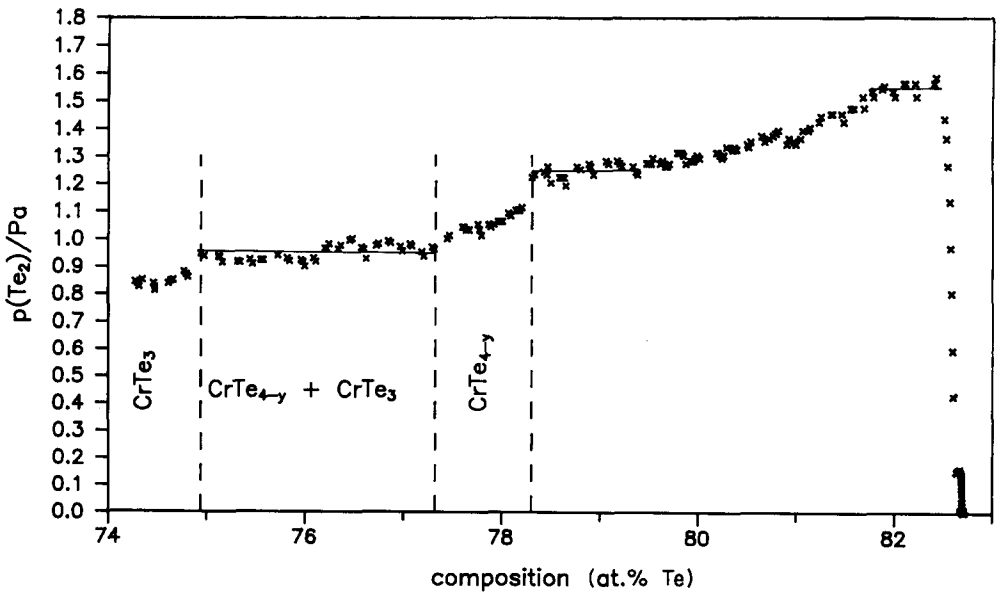

Fig. 3. $p(Te_2)$ as a function of composition; deduced from $I(\mathrm{Te_2}^+)\sqrt{T}$–time plot shown in Fig. 1, and eqn. (5); $T = 650$ K.

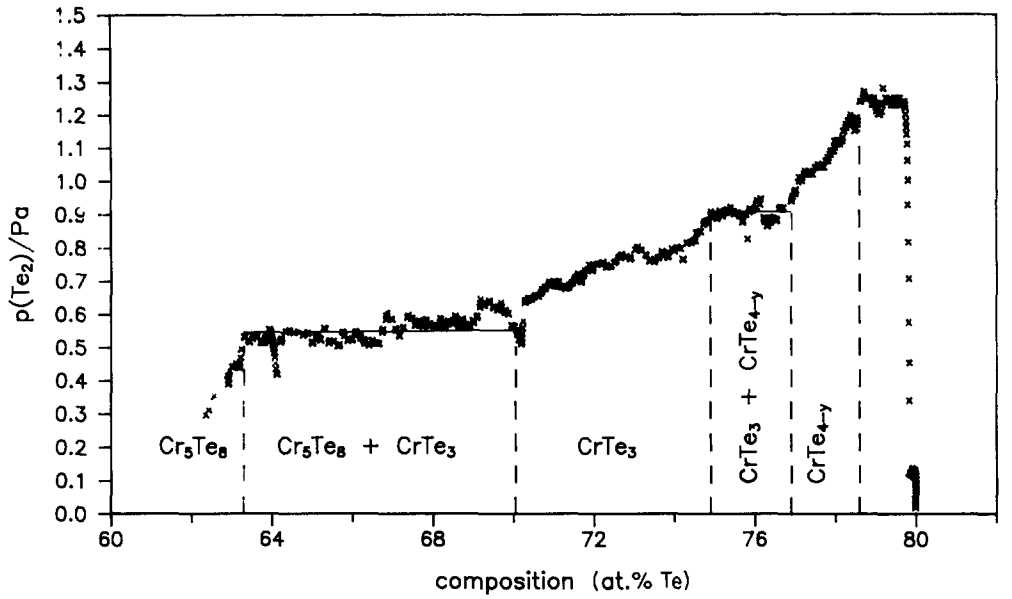

Fig. 4. $p(Te_2)$ as a function of composition; deduced from $I(Te_2^+)\sqrt{T}$–time plot shown in Fig. 2, and eqn. (5); $T = 650$ K.

TABLE 1. Te-rich and Cr-rich boundary compositions (in at.% Te) of the single-phase regions[a] identified in the Te-rich part of the Cr–Te phase diagram (>62 at.% Te)

Run	$CrTe_{4-y}$		$CrTe_3$		Cr_5Te_8
	Te-rich boundary	Cr-rich boundary	Te-rich boundary	Cr-rich boundary	Te-rich boundary
Initial composition of the sample: 82.7 at.% Te					
1	78.1	77.0	74.2	71.2	
2	78.3	77.3	74.8		
3	78.3	77.4			
Initial composition of the sample: 80.0 at.% Te					
4			73.7	70.9	63.8
5	78.4	76.7	74.6	70.2	63.6
6	78.5	76.8	74.9	69.5	62.5
Initial composition of the sample: 70.1 at.% Te					
7[b]					63.5
8					64.3
Initial composition of the sample: 66.9 at.% Te					
9					63.6
Selected[c] (Mean):	78.3±0.2	77.0±0.3	74.4±0.5	70.5±0.8	63.6±0.6

[a] $CrTe_{4-y}$: tentative formula assigned by us for the hitherto unknown single-phase; $CrTe_3$ and Cr_5Te_8: formulae assigned by Ipser *et al.* [6] retained.
[b] Except in this run ($T = 688$ K), the phase boundary compositions given in this table all correspond to $T = 650$ K.
[c] Errors quoted are standard deviations of the mean values.

$$\log[p^\circ(Te_2)/Pa)] = -(7781 \pm 84)(K/T) + (12.155 \pm 0.132) \quad (7)$$

By a Gibbs–Duhem integration, the activities of chromium were also deduced. The partial molar Gibbs free energies of Cr and Te in the Cr–Te alloys (at $T = 650$ K) and consequently their Gibbs free energies of formation were then computed. Table 2 gives the $\Delta_f G_m^\circ$ values corresponding to the Cr-rich and/or Te-rich boundary compositions.

Figure 5 shows the $I(Te_2^+)\sqrt{T}$–time plot, obtained in one of the vaporization experiments, in which a sample with the starting composition of 80 at.% Te was vaporized at different temperatures such that finally the $(Cr + CrTe_x)$ two-phase field could be reached. Figure 6 shows the corresponding $p(Te_2)$–composition plot (Fig. 6(a): 80–50 at.% Te; Fig. 6(b): 63–50 at.% Te). Vaporization through the intermediate region, 63–50 at.% Te (see Fig. 6(b)), was carried out mainly to examine whether any information about the constitution of this part of the Cr–Te phase diagram could be obtained.

4. Discussion

We did not label the region between the plateau at ~1.5 Pa and that at ~1.2 Pa (see Fig. 3) as that of the most Te-rich phase in the Cr–Te system because the first plateau was for a rather small duration and the difference between $p^\circ(Te_2) = 1.5$ Pa and $p(Te_2) = 1.2$ Pa was also not well beyond the uncertainty level in our pressure measurements. Investigations with samples having tellurium content higher than 82.7 at.% Te are necessary to confirm whether or not the drop from 1.5 Pa to 1.2 Pa is real.

The composition region between plateau 2 (~1.2 Pa) and plateau 3 (~0.9 Pa) is assigned to a hitherto unknown polytelluride phase to which we have given a tentative formula, $CrTe_{4-y}$ (from 77±0.3 to 78.3±0.2

TABLE 2. $\Delta_f G_m^\circ$ (650 K)[a] (in kJ mol^{-1}) for Te-rich chromium tellurides; reference states: Cr(s), Te(s)

Sample composition used (at.% Te)	Te-rich boundary		Cr-rich boundary	
	formula	$\Delta_f G_m^\circ$	formula	$\Delta_f G_m^\circ$
For the phase, $CrTe_{4-y}$				
82.7[b]	$CrTe_{3.57}$	−91.0	$CrTe_{3.35}$	−90.8
	$CrTe_{3.61}$	−91.0	$CrTe_{3.41}$	−90.8
	$CrTe_{3.61}$	−90.8	$CrTe_{3.42}$	−90.6
80.0[c]	$CrTe_{3.63}$	−90.8	$CrTe_{3.29}$	−90.5
	$CrTe_{3.65}$	−90.0	$CrTe_{3.31}$	−89.7
Selected (mean)[d]:				
	$CrTe_{3.61}$	−90.7 ± 0.4	$CrTe_{3.35}$	−90.5 ± 0.4
For the phase, $CrTe_3$				
82.7[b]	$CrTe_{2.88}$	−90.3	$CrTe_{2.47}$	−89.6
	$CrTe_{2.97}$	−90.3		
80.0[c]	$CrTe_{2.80}$	−92.1	$CrTe_{2.44}$	−91.4
	$CrTe_{2.94}$	−90.0	$CrTe_{2.36}$	−88.8
	$CrTe_{2.98}$	−89.3	$CrTe_{2.28}$	−88.1
Selected (mean)[d]:				
	$CrTe_{2.91}$	−90.4 ± 1.0	$CrTe_{2.39}$	−89.5 ± 1.5
For the phase, Cr_5Te_8				
80.0[c]	$CrTe_{1.76}$	−89.4		
	$CrTe_{1.75}$	−87.2		
	$CrTe_{1.67}$	−86.2		
70.1[e]	$CrTe_{1.80}$	−84.0		
66.9[e]	$CrTe_{1.75}$	−84.3		
Selected (mean)[d]:				
	$CrTe_{1.75}$	−86.2 ± 2.2		

[a]Computed from Te activities (determined in this study) and Cr activities (deduced by using Gibbs–Duhem integration) at $T = 650$ K; the activity values used are those corresponding to the phase boundary compositions.

[b]$a_{Cr} = 4.2 \times 10^{-8}$ [2] at compositions >82 at.% Te (plateau 1 where $p(Te_2) = 1.5$ Pa and $a_{Te} = 1$) was used as a starting point for all Gibbs–Duhem computations.

[c]$a_{Cr} = 7.9 \times 10^{-8}$ was employed as the starting point for Gibbs–Duhem computations; this value corresponding to plateau 2 (*i.e.* the constant $p(Te_2)$ region: 78.3–79.2 at.% Te in which $p(Te_2) = \sim 1.2$ Pa) was deduced from the results obtained in the experiments with the 82.7 at.% Te sample.

[d]Errors quoted are standard deviations of the mean values.

[e]$a_{Cr} = 2.4 \times 10^{-7}$ (between 63.6 and 70.5 at.% Te) was employed as the starting point for Gibbs–Duhem calculations; this value corresponding to plateau 4 (*i.e.* the constant pressure region: 63.6–70.5 at.% Te where $p(Te_2) = \sim 0.55$ Pa) was deduced from the results obtained in experiments with the 80.0 as well as the 82.7 at.% Te samples.

at.% Te). A compound of this composition does not appear to have been reported in the literature. Plateau 2 and plateau 3 not only remained for reasonably long periods, but were also obtained in experiments with different samples (82.7 and 80.0 at.% Te).

We have ascribed the compositional dependence of $p(Te_2)$ from 70.5 ± 0.8 to 74.4 ± 0.5 (*i.e.* between plateau 3 and plateau 4) to the phase $CrTe_3$, identified first by Ipser and coworkers [4–6]. The phase diagram [6] proposed by these authors show a much narrower width (from 74 to 74.9 at.% Te) for this phase. They envisaged two other possibilities as well (neither of which was incorporated in the phase diagram):

(a) the homogeneity range of $CrTe_3$ might even start from 71 at.% Te; and

(b) a new phase with a narrow homogeneity range might exist at 70 at.% Te. Our result is in accord with the former.

Plateau 4 (~0.55 Pa) is quite long enough and clearly represents a biphasic region. By assuming this region to correspond to ($Cr_5Te_8 + CrTe_3$), we deduced the Te-rich boundary of the Cr_5Te_8 phase as 63.6 ± 0.6 at.% Te, which is more Te-rich than that (~62 at.% Te) proposed by Ipser *et al.* [6].

Our results do not support the hypothesis of Gunia [3] that at $T < 700$ K, the composition range above 60 at.% Te consists of two biphasic regions, namely, ($Cr_2Te_3 + Cr_3Te_8$) and ($Cr_3Te_8 + Te$), separated by a narrow single phase (Cr_3Te_8) region at ~72.5 at.% Te.

The results (run 4, Table 1) deduced from the experiment which involved continuous vaporization of a sample from ~80.0 to as low as 49.6 at.% Te (see Figs. 5 and 6) are consistent with the rest where the final compositions were generally well above 60 at.% Te. The Cr-rich boundary of the most Cr-rich telluride obtained in this experiment at $T = 1120$ K (~50 at.% Te) was also in agreement with that obtained earlier [1] from samples having initial tellurium contents only of 55.6 and 57.2 at.%. These were taken to indicate reliability of the boundary compositions reported here.

This particular experiment has also served to show that at $T > 900$ K, the intermediate region of the Cr–Te phase diagram (from 50 to ~62 at.% Te) is not likely to consist of any two-phase regions with significant width. The $p(Te_2)$ (see Fig. 6(b)) never really remained constant except when the sample had entered the $Cr + CrTe_x$ two-phase field. It needs to be mentioned here, however, that the entire composition range was not traversed at a single temperature in this experiment. At low temperatures, vapor pressures became too low (after the sample composition reached a value of ~60 at.% Te) to permit composition changes in reasonable time. One cannot possibly effect the cross-over at a single high temperature without violating the Knudsen flow conditions, at least at some point.

The mass loss and thus the sample compositions which eqns. (4) and (5) can yield will be exactly the same (even if Te_2 is not the major vapor species) provided the value of $\Sigma_i Q_i$ remains unchanged throughout the duration of an experiment. The way in which c_2 or c_2' is deduced ensures a higher value for c_2' which in turn suitably compensates for the non-inclusion of the $\Sigma_i Q_i$ term in eqn. (5). $c_2' > c_2$ since $c_2' = c_2(1 + \Sigma_i Q_i)$.

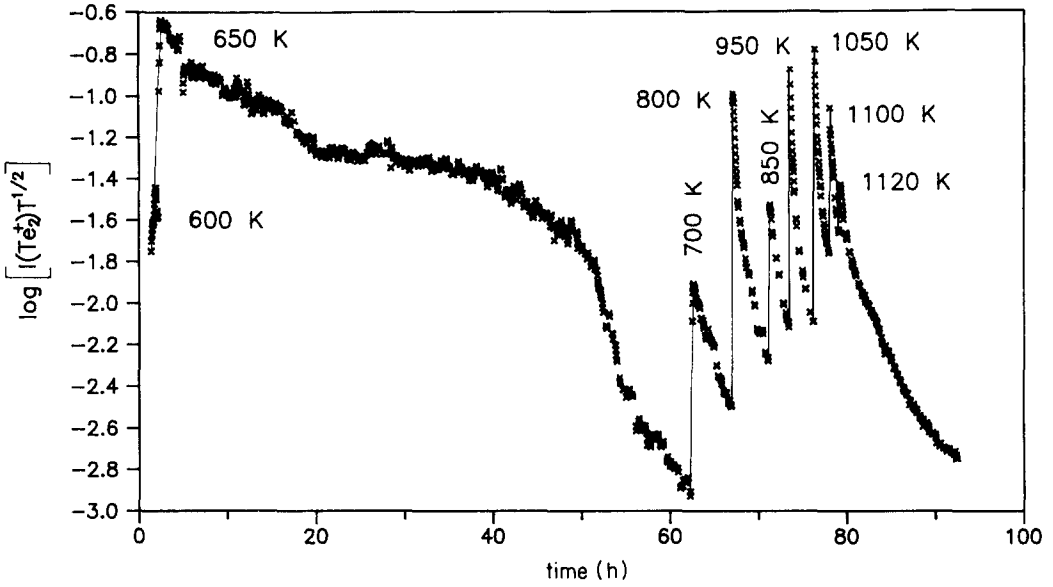

Fig. 5. $I(Te_2^+)$ as a function of time; starting composition of the sample: 80.0 at.% Te; initial weight: 0.198 29 g; total mass loss: 0.135 61 g.

However, the compensation may not be adequate when $\Sigma_i Q_i$ changes with time, as can happen if vaporization is not conducted at a single temperature and/or if the sample alternately traverses through single- and two-phase regions. The mass loss might be overestimated or underestimated depending on whether $(1+\Sigma_i Q_i)$ at a given point was less than or greater than c_2'/c_2. The resulting error in the composition will then be insignificant only if $\Sigma_i Q_i$ is negligibly small, that is, if the mole fraction of the tellurium dimer is far higher than those of other tellurium species. That for elemental tellurium the mole fraction of Te_2 is as high as 0.95 (at $T=650$ K) [9–12] has long been known. To understand the situation in the case of an alloy system, the following pressure-independent equilibria may be examined:

$$Te_2(g) + (i\text{-}2)Te(\text{in condensed phase}) = Te_i(g) \quad (8)$$

The equilibrium constant for this reaction is

$$K_i = [p(Te_i)/p(Te_2)]/[a_{Te}]^{(i-2)} \quad (9)$$

When $a_{Te}=1$, $K_i=[p^\circ(Te_i)/p^\circ(Te_2)]$, where the superscript "o" represents the value over elemental tellurium. Hence the above equation can be rearranged to

$$[p(Te_i)/p(Te_2)] = [p^\circ(Te_i)/p^\circ(Te_2)][a_{Te}]^{(i-2)} \quad (10)$$

The above relation clearly brings out the decreasing importance of Te_i $(i>2)$ with a decrease in tellurium activity. Thus the mole fraction of Te_2 in any alloy system can only be higher than that over elemental tellurium unless the a_{Te} is so low (or the temperature so high) that monomer tellurium can become an equally [1] or even a more dominant [13] species in the vapor phase.

We have, in fact, confirmed by means of actual calculations (in the case of a run shown in Figs. 2 and 4) that the maximum difference between the compositions deduced from eqn. (5) and those from eqn. (4) is no more than 0.08 at.%. Te (observed at ~71 at.% Te, corresponding to ~64% of total mass loss and ~55% of total time). The $I(Te_i^+)$ where $i=3$–7, required in these calculations, were deduced from the measured $I(Te_2^+)$ and other pertinent data. Obviously, the term $\Sigma_i Q_i$ in eqn. (4) is negligibly small when the composition lies at >63 at.% Te.

In the experiment which involved evaporation at high temperatures (see Fig. 5), however, mass loss due to effusion of monomeric tellurium species might not be negligible. Calculations according to eqns. (4) and (5) showed that the two sets of values differ by as much as ~1.0 at.% Te (observed at ~54 at.% Te, corresponding to ~94% of total mass loss and ~83% of total vaporization time). The $I(Te^+)$ necessary for use in eqn. (4) was deduced from the measured $p(Te_2)$ and the known dissociation constant of $Te_2(g)$ [14]. The compositions shown in Fig. 6 correspond to those obtained by using eqn. (4).

Our Gibbs–Duhem calculations had its starting point at the most Te-rich two-phase region where $a_{Te}=1$. A value of $a_{Cr}=4.2\times10^{-8}$ at $T=650$ K, estimated from the results of Goncharuk and Lukashenko [2], was assigned to this phase field. Although these authors chose to give a single electromotive force (e.m.f.)–temperature relation for the entire composition range from 65 to 88.6 at.% Te, the figure given by them

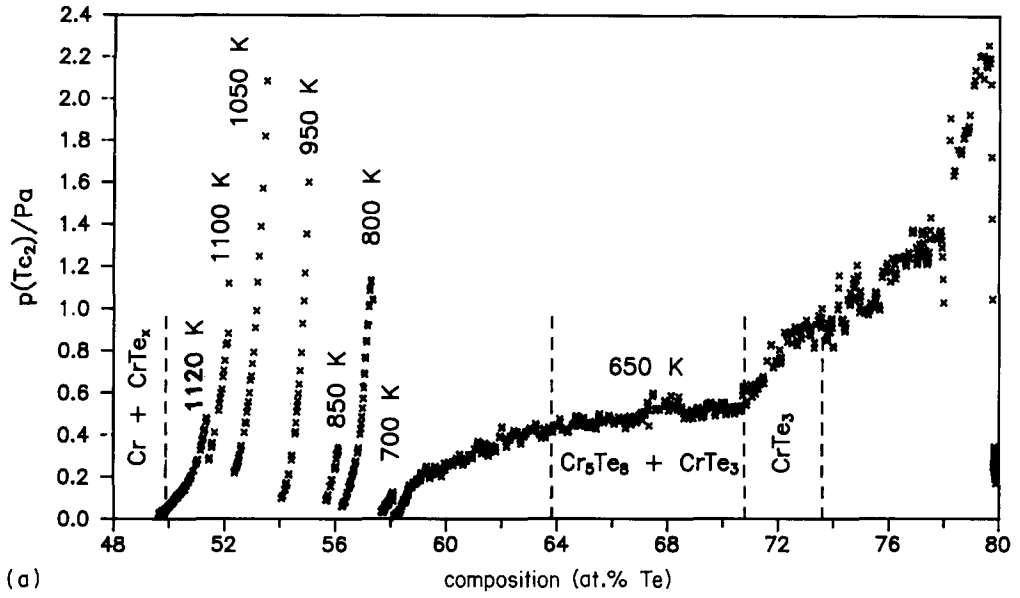

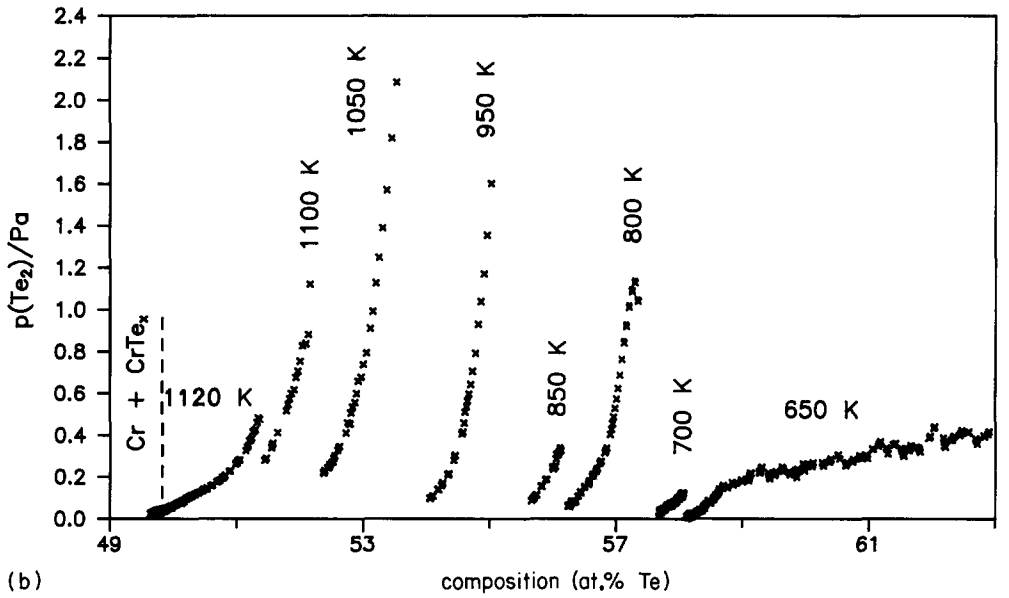

Fig. 6. (a) $p(Te_2)$ as a function of composition; deduced from $I(Te_2^+)\sqrt{T}$–time plot shown in Fig. 5, and eqn. (4). (b) $p(Te_2)$ as a function of composition in the intermediate part of the Cr–Te phase diagram (part of Fig. 6(a)).

reveals a trend: the higher the tellurium concentration the higher are the e.m.f. values and the difference is at least ~20 mV. In view of this, we added 10 mV to the e.m.f. value (455.4 mV at $T=650$ K) calculated from the reported least-squares-fit relation to derive the aforementioned a_{Cr}.

The a_{Cr} deduced for the biphasic region $Cr_5Te_8+CrTe_3$ is ~5.7 times that we assigned for compositions >82 at.% Te. This corresponds to a difference of ~48 mV, whereas the figure given by Goncharuk and Lukashenko [2] shows a maximum difference of only about 30 mV.

The integral Gibbs free energies of formation, given in Table 2 for various Te-rich phases, indicate that the changes in $\Delta_f G_m°$ are rather small. A similar observation was also made previously by Ipser *et al.* [5], who estimated the Gibbs free energies of formation (at $T=668$ K) for the phases $CrTe_3$, $Cr_{1.3}Te_3$ and Cr_5Te_8: -90.2 kJ mol^{-1} ($CrTe_{2.92}$; 74.5 at.% Te), -90 kJ mol^{-1} ($CrTe_{2.33}$; 70 at.% Te) and -89.5 kJ mol^{-1} ($CrTe_{1.63}$; 62 at.% Te).

Small differences in the $\Delta_f G_m°$ values stem from rather small changes in the activities of Te and Cr across the composition range above 63.6 at.% Te. As

we go from the most Te-rich two-phase region to $Cr_5Te_8 + CrTe_3$, the a_{Te} decreases from 1 to ~0.6 while the a_{Cr} (as obtained from our Gibbs–Duhem calculations) increases from 4.2×10^{-8} to 2.4×10^{-7}. Under such a situation, one might fail to detect compositional dependence of activities, especially if they are measured only at a few sample compositions. It is in this particular aspect that the method used in the present study offers a great advantage. Numerous compositions could be generated *in situ* and the activities for all these compositions could be deduced. For instance, data shown in Fig. 3 correspond to about 170 compositions (composition range: from 82.7 to 74.3 at.% Te) while those shown in Fig. 4 correspond to as many as 570 compositions (composition range: from 80.0 to 62.3 at.% Te). Furthermore, since experiments with samples of different starting compositions can give rise to several common compositions, the method also provides a means of ascertaining that the activities assigned to these compositions do represent the equilibrium values.

The powder X-ray diffraction patterns of all Cr–Te samples were not only complex but revealed many weak lines. Information about only some major peaks are given in Table 3.

Both 82.7 and 80.0 at.% Te samples showed some lines close to those obtained with tellurium. This suggests that both samples correspond to the same two-phase field, *i.e.* (Te + most Te-rich chromium telluride). However, not all lines other than those due to tellurium are common.

TABLE 3. X-ray diffraction results for tellurium and the Cr–Te alloys used in our investigations. Only data for the major peaks are tabulated

Sample composition (at.% Te)	*d*-spacing (Å)[a]
100	3.232_x, 2.347_4, 2.226_3, 3.83_2, 1.83_2; $x=240$ cm
82.7	3.235_x, 2.987_4, 3.399_3, 2.350_3, 2.350_3, 2.228_2, 1.873_1; $x=500$ cm
80.0	3.240_x, 3.473_7, 2.888_6, 2.351_3, 2.229_2, 3.28_1, 1.86_1; $x=170$ cm
70.1	3.470_x, 2.891_2, 2.940_2, 3.008_2, 6.945_1, 3.033_1, 1.944_1, 1.734_1; $x=320$ cm
66.9	2.942_x, 3.010_7, 3.036_6, 2.894_6, 3.44_5, 2.241_3, 3.36_3, 1.63_2; $x=140$ cm
64.2[b]	2.948_x, 2.990_7, 2.888_6, 1.573_6, 2.242_4, 1.952_4, 3.413_3, 3.230_3, 1.872_2, 3.468_2; $x=80$ cm
74.3[b]	2.890_x, 3.476_4, 2.995_3, 1.873_2, 3.414_2, 1.946_2, 3.239_2, 1.926_2, $x=90$ cm
74.2[b]	2.993_x, 3.410_8, 2.892_5, 1.875_5, 3.474_2, 1.663_2, 2.94_1; $x=170$ cm

[a] x denotes the biggest peak; subscripts denote relative peak heights in percentages (2, for instance, refers to the 20% peak); height of the 100% peak (x) is also given.
[b] Compositions at the end of vaporization experiments with the 82.7 at.% Te samples (*i.e.* after runs 1, 2, 3 of Table 1).

The patterns of the samples with 66.9 and 70.1 at.% Te were more or less similar. No lines resulting from tellurium or chromium were seen in these patterns. From a comparison of the peak heights of the common lines in the patterns of these two samples, the following inferences could be made:

(a) the lines at $d=6.945$, 3.470 and 1.734 Å may be characteristic of the $CrTe_3$ phase

(b) the line at $d=3.036$ Å might be representative of the Cr_5Te_8 phase;

(c) as for the other common lines, only very tentative assignment can be thought of – those lines observed at $d=3.36$, 3.010, 2.942 and 2.241 Å probably represent the Cr_5Te_8 phase and those at $d=2.891$ and 1.944 Å the $CrTe_3$ phase.

None of the *d*-values assigned for the $CrTe_3$ phase differs by more than 0.005 Å from the values calculated by using the lattice parameter data reported by Ipser *et al.* [6] for the same phase. In the case of the *d*-values assigned for Cr_5Te_8, agreement with the calculated values (using the X-ray data of Ipser *et al.* [6]) was not so good.

The diffraction patterns of 74.3 and 74.2 at.% Te samples (residues) were similar. Both these compositions should correspond to $CrTe_3$. However, for two of the five major peaks, our values ($d=2.995$ or 2.993 Å, and 3.414 and 3.410 Å) differ by as much as ~0.01 Å from those derived (3.013 and 3.402 Å) for $CrTe_3$ [6].

The pattern of the other residue (64.2 at.% Te) was similar to those obtained for 66.9 and 70.1 at.% Te samples. The biggest peaks for both 66.9 and 64.2 at.% Te compositions are seen at and around the same *d*-spacing value of ~2.94 Å.

5. Conclusions

A hitherto unknown polytelluride $CrTe_{4-y}$ (77–78.3 at.% Te) has been identified. Although indications for the existence of one more polytelluride phase on the Te-rich side of $CrTe_{4-y}$ were obtained, further studies are clearly necessary to confirm this. The uncertainty regarding the homogeneity range of $CrTe_3$, hitherto considered as the novel and the most Te-rich phase in the Cr–Te system [6] was removed. This phase exists from 70.5 to 74.4 at.% Te. The Te-rich boundary of Cr_5Te_8 (63.6 at.% Te) is slightly more Te-rich than that (62 at.% Te) suggested by Ipser *et al.* [6]. The intermediate part of the Cr–Te phase diagram (between 50 and 62 at.% Te) at $T>900$ K is not likely to consist of any two-phase region with significant width. A redetermination of Cr activities (at as many compositions as possible) in the Te-rich region is desirable.

Acknowledgments

The authors thank the X-ray group (Mr. K.V.G. Kutty, Dr. S. Rajagopalan and Mr. R. Asuvathraman) for their generous help in the characterization of the samples and for useful discussions; they also wish to thank the electronics group (Mr. K.C. Srinivas, Mr. R. Parthasarathy and Ms B. Suhasini) for maintenance of the mass spectrometer.

References

1 R. Viswanathan, M. Sai Baba, D. Darwin Albert Raj, R. Balasubramanian, B. Saha and C.K. Mathews, *J. Nucl. Mater., 167* (1989) 94.
2 L.V. Goncharuk and G.M. Lukashenko, *Sov. Powder Metall. Met. Ceram., New York, 13* (1974) 726.
3 P.G. Gunia, *Thesis,* Gesamthochschule Siegen, 1979.
4 K.O. Klepp and H. Ipser, *Monatsh. Chem., 110* (1979) 499.
5 H. Ipser, K.O. Klepp and K.L. Komarek, *Monatsh. Chem., 111* (1980) 761.
6 H. Ipser, K.L. Komarek and K.O. Klepp, *J. Less-Common Met., 92* (1983) 265.
7 M. Sai Baba, R. Viswanathan, R. Balasubramanian, D. Darwin Albert Raj, B. Saha and C.K. Mathews, *J. Chem. Thermodyn., 20* (1988) 1157.
8 R. Viswanathan, D. Darwin Albert Raj, T.S. Lakshmi Narasimhan, R. Balasubramanian and C.K. Mathews, *J. Chem. Thermodyn., 25* (1993) 533.
9 R. Viswanathan, *Ph.D. Thesis: Studies on Binary Systems of Tellurium with Chromium and Molybdenum by Using Knudsen Effusion Mass Spectrometry,* University of Madras, 1991.
10 A. Neubert, *High Temp. Sci., 10* (1978) 261.
11 F. Grønvold, J. Drowart and E.F. Westrum, Jr., *The Chemical Thermodynamics of Actinide Elements and Compounds, Part 4: The Actinide Chalcogenides (Excluding Oxides),* IAEA, Vienna, 1984.
12 R. Viswanathan, M. Sai Baba, D. Darwin Albert Raj, R. Balasubramanian and C.K. Mathews, in J.F.J. Todd (ed.), *Advances in Mass Spectrometry Part B,* John Wiley & Sons, Chichester, 1986, p. 1087.
13 M. Sai Baba, T.S. Lakshmi Narasimhan, R. Balasubramanian and C.K. Mathews, *J. Nucl. Mater., 201* (1993) 147.
14 R. Viswanathan, M. Sai Baba, D. Darwin Albert Raj, R. Balasubramanian, T.S. Lakshmi Narasimhan and C.K. Mathews, *Spectrochim. Acta B: Atom. Spectrosc.,* in press.